Japanese Journal of Applied Physics

BRIEF NOTE

High-speed photography of gas release from bioactive glass

To cite this article: Michiel Postema *et al* 2024 *Jpn. J. Appl. Phys.* **63** 028001

Japanese Journal of Applied Physics **63**, 028001 (2024) **BRIEF NOTE**
https://doi.org/10.35848/1347-4065/ad1bc2

High-speed photography of gas release from bioactive glass

Michiel Postema[1,2*], Craig S. Carlson[1,2], Nicole Anderton[1], Hu Xinyue[3], Momoka Yamasaku[3], Laeticia Petit[4], Jonathan Massera[1], and Nobuki Kudo[3]

[1]*BioMediTech, Faculty of Medicine and Health Technology, Tampere University, Korkeakoulunkatu 3, FI-33720 Tampere, Finland*
[2]*School of Electrical and Information Engineering, University of the Witwatersrand, Johannesburg, 1 Jan Smuts Laan, 2001 Braamfontein, South Africa*
[3]*Faculty of Information Science and Technology, Hokkaido University, Kita 14 Jo, Nishi 9 Chome, Kita-ku, Sapporo, Hokkaido 060-0814, Japan*
[4]*Photonics Laboratory, Faculty of Engineering and Natural Sciences, Tampere University, Korkeakoulunkatu 3, FI-33720 Tampere, Finland*

[*]E-mail: michiel.postema@tuni.fi

Received November 15, 2023; revised December 27, 2023; accepted January 4, 2024; published online January 19, 2024

Bioactive glass has been of interest for applications in bone regeneration. Floating bioactive glass particles were observed to sink in ultrasound. The purpose of this study was to qualify and quantify bubble formation from floating bioactive glass particles. Water droplets containing borosilicate glass 13-93B20 particles, where 20% of the SiO_2 was replaced with B_2O_3, of dimensions <38 μm were subjected to pulsed ultrasound, whilst being video-recorded at high speed. Measured radial expansions >20 μm corresponded to cavitation nuclei of initial radius 0.6 μm. This study provides experimental evidence that gas trapped inside bioactive glass may be released using high-amplitude ultrasound pulses.

Bioactive glass is a class of biomaterials that has been of interest for applications in bone regeneration.[1)] Borosilicate glasses have been found not only to promote osteogenesis but also angiogenesis.[2)] The borosilicate glass 13-93B20, where 20% of the SiO_2 was replaced with B_2O_3, has been the object of prior research.[3,4)] Despite its high density of 2.60 g cm^{-3} at RT, approximately 9% of microscopic 13-93B20 particles have been observed to float on water.[4)] This floating has been attributed to gas entrapment inside the particles.[4)]

Subjecting floating 13-93B20 particles to ultrasound pulses with a centre frequency of 1 MHz forces them to sink.[4)] The purpose of this study was to investigate any cavitation phenomena during sonication of 13-93B20 particles, with special attention to gas release.

Let us assume a microscopic spherical gas bubble in an infinite fluid. If the bubble is subjected to an ultrasound pulse, its radial response can be expressed by a Rayleigh–Plesset equation.[5–7)] For the purposes of this study, we may ignore nonspherical terms and multiple scattering,[8–10)] as we concentrate on the first pulsation cycles. A simplified equation for ultrasound-driven microbubble pulsation has been derived in a prior publication,[11)] and modified to incorporate viscous, reradiation, and thermal damping terms.[12)] If the kinetic energy of the gas–liquid bubble interface surpasses its surface energy,[13)] bubble fragmentation may occur during the contraction phase.[14)] Bubble fragmentation is followed by coalescence of fragments during the expansion phase.[15)] The asymmetric collapse of a bubble may lead to the formation of a liquid jet.[16–20)] Liquid jet occurence has been associated with the generation of shock waves,[21)] as well as the production of free radicals and heat.[22–24)]

To numerically simulate pulsations of released gas, solutions of the Rayleigh–Plesset equation were computed using the ode45 differential equation solver of MATLAB® (The MathWorks, Inc., Natick, MA, USA) for initial bubble radii between 0.1 μm and 5.0 μm.[25)] Bubble radii were plotted as a function of time, a so-called $R(t)$ curve.

Experiments were performed on borosilicate glass 13-93B20 particles <38 μm that had been prepared as preciously reported.[3,4)] Quantities of 5 mg of these particles were stirred though 5 ml of degassed distilled water (FUJIFILM Wako Pure Chemical Corporation, Chuo-ku, Osaka, Japan). For each experiment, 200 μl of this dispersion was pipetted into the observation compartment that was part of the high-speed photography system presented in a separate study.[26)] In short, the compartment was part of a water-filled Perspex container positioned on top of an Eclipse Ti inverted microscope (Nikon Corporation, Minato-ku, Tokyo, Japan) with either a Plan Apo LWD 10×/0.45 objective lens (Nikon), a 1.5× internal zoom, and a G-2A filter, or an S Plan Fluor ELWD 40×/0.6 objective lens (Nikon). The objective lens was focused on the top of the compartment with floating bioactive glass particles. The top of the compartment restrained the particles from floating farther up, but introduced a reflective interface distal to the particles. The microscope was attached to an HPV-X2 high-speed camera (Shimadzu, Nakagyo-ku, Kyoto, Japan), operating at a frame rate of ten million frames per second during sonication of the sample droplet in the observation compartment.

The ultrasound was produced by generating a 3-cycle pulse at a centre frequency of 1 MHz with an AFG320 arbitrary function generator (Sony-Tektronix, Shinagawa-ku Tokyo, Japan) that was amplified by a UOD-WB-1000 wide-band power amplifier (TOKIN Corporation, Shiroishi, Miyagi, Japan) and fed into a custom-built focused single-element transducer.[26)] Signal amplitudes varying from 0.200 to 5.00 V were used. These amplitudes corresponded nonlinearly to peak-negative pressures between 40 kPa and 1.30 MPa in a situation without reflectors.

A total number of 67 high-speed videos was recorded, each composed of 256 frames. These frames were processed in MATLAB® to measure bubble radii as a function of time. The simulated $R(t)$ curves were then superimposed on the experimental data using a laborious manual fitting protocol in MATLAB® and assuming perfect reflection from the nearest interface.

Bubble activity was only observed when applying peak voltages of 5 V.

Figure 1 shows a sequence of high-speed video frames of gas nucleating from a bioactive glass particle, overlain on a numerically simulated $R(t)$ curve. A bubble was measured to expand to a radius of 17 μm. Following subsequent collapse, its fragments were seen to expand to a blob spanning an area with a radius of 24 μm. After another collapse, micron-sized nonpulsating entities were observed to float in proximity to the bioactive glass particle. These entities may have been fragments

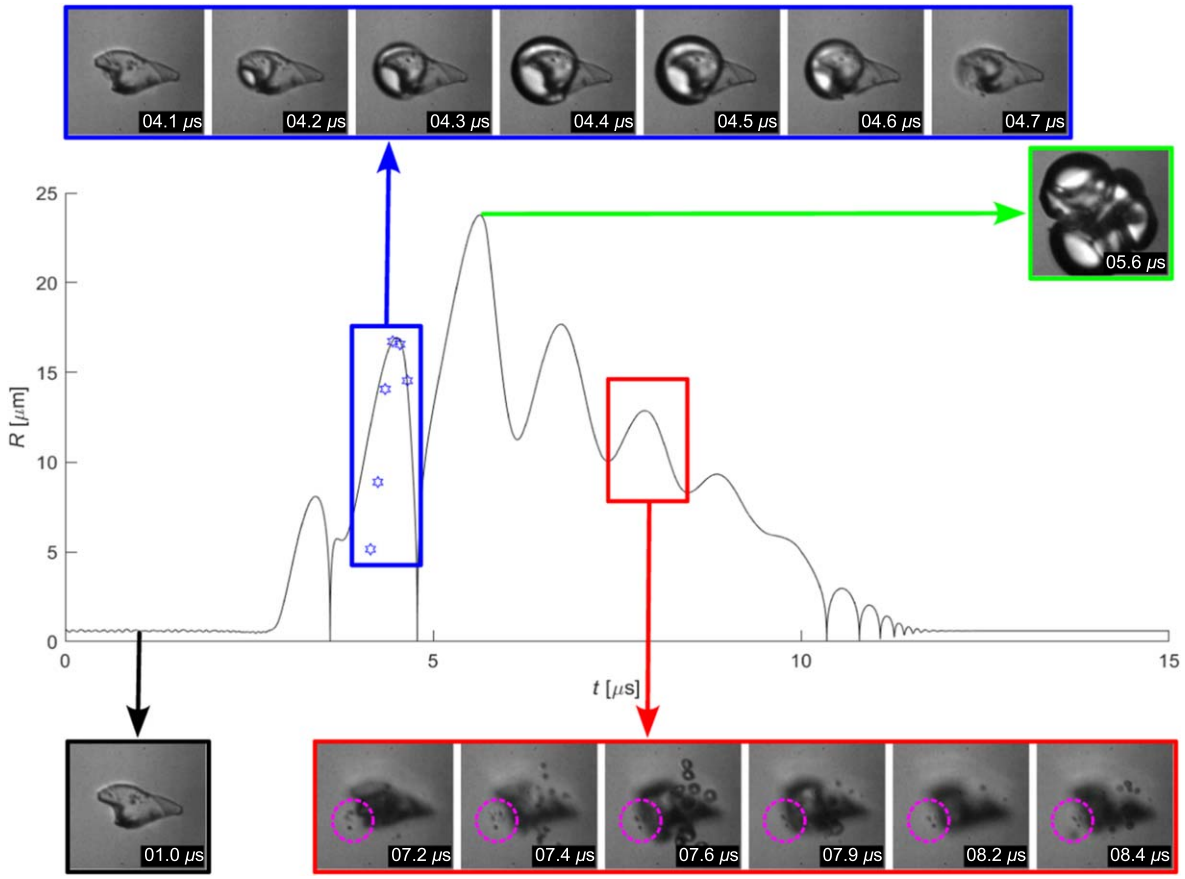

Fig. 1. Selected frames from a high-speed imaging sequence recorded at ten million frames per second, overlain on a simulated $R(t)$ curve of a gas microbubble of initial radius $R(0) = 0.6$ μm. Floating non-pulsating chips have been indicated by magenta circles. Each frame corresponds to an area of 65×60 μm^2. Timestamps have been added to the lower right corners.

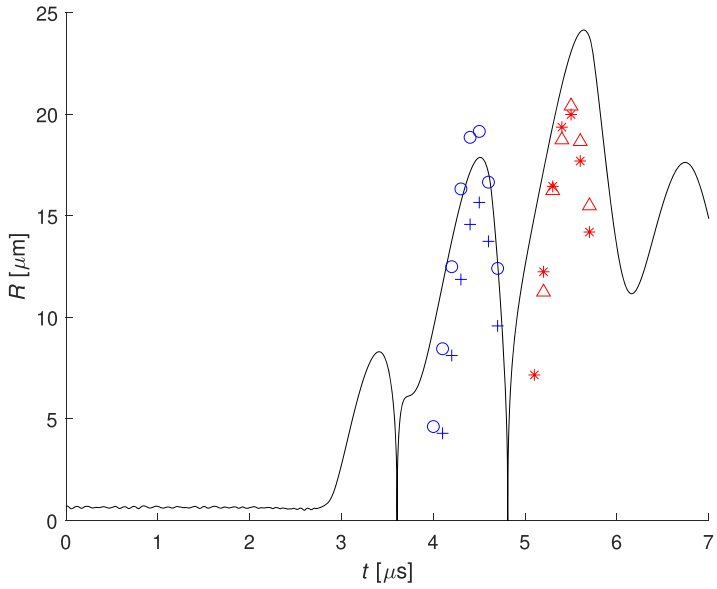

Fig. 2. Radius as a function of time measured for two released bubbles (△,*) and two inertial cavities (∘,+) measured from high-speed image frames (overlain) and simulated for a gas nucleus of initial radius $R(0) = 0.6$ μm (—).

chipped off from the glass particle. No visible changes in particle size or shape were observed during and after sonication. The glass particle itself shifted out of focus, indicating its sinking. In subsequent videos (not shown) the glass particle was not visible, indicating a permanent sunken state.

To find the source of the nucleating gas, $R(t)$ curves were computed to match nucleation near bioactive glass particles. Figure 2 shows data points of the measured bubble excursions resulting from sonicating two bioactive glass particles in a high-speed experiment and simulated $R(t)$ curves fitting through those points. The experiments themselves are not shown here. In the experiments, no cavitation activity in or on the glass was observed during the first sonication cycle, as opposed to inertial cavitation activity in a separate experiment.

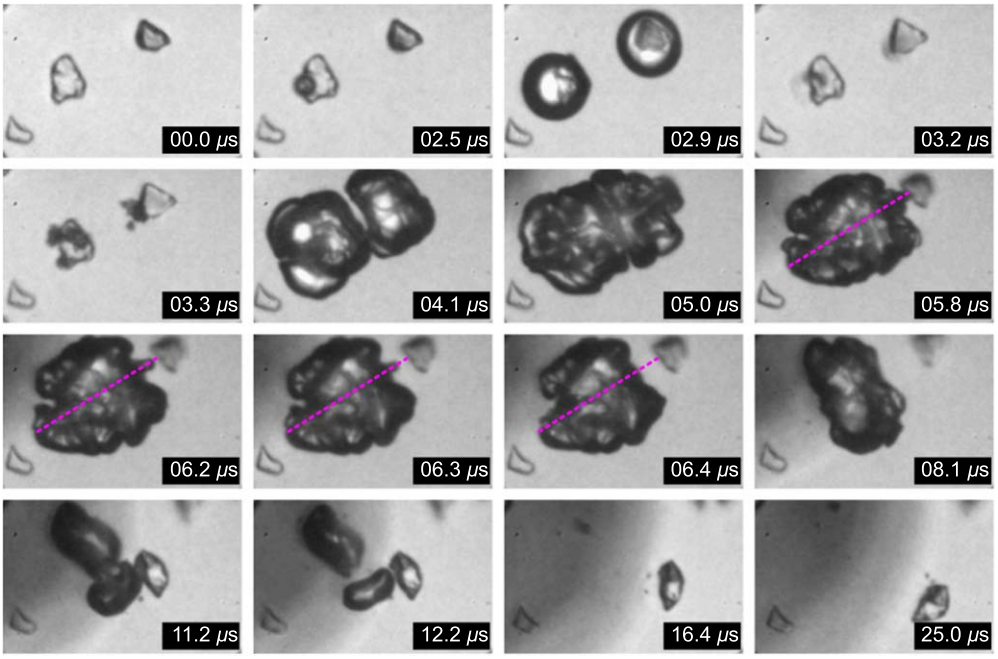

Fig. 3. Selected frames from a high-speed imaging sequence. The formation of a needle jet is visible, whose axis indicated by a dashed magenta line (- - -). Each frame corresponds to an area of 140 × 90 μm^2. Timestamps have been added to the lower right corners.

During the second sonication cycle, radial excursions were observed that matched simulated excursions of a gas nucleus of initial radius $R(0) = 0.6$ μm. Such a nucleus would have had an excursion amplitude of 5 μm during the first sonication cycle. As any such cavitation activity was not visible near or on both bio-active glass particles, we presume the gas was released from within the bioactive glass.

Figure 3 shows selected high-speed video frames of simultaneous gas release from two bioactive glass particles, at time $t = 2.5$ μs after the start of the experiment, maximum expansion at $t = 2.9$ μs, collapse and fragmentation at $t = 3.2$ μs, expansion of fragments at $t = 3.3$ μs, coalescence of fragments at $t = 4.1$ μs, drainage of a liquid film separating the two bubble entities at $t = 5.0$ μs, jetting between $t = 5.8$ μs and $t = 6.3$ μs, leading to a split-up into two parts at $t = 11.2$ μs. A glass particle was seen to rotate and drift away after final collapse of the gas bubbles. The phenomena described have been described for free and lipid-encapsulated bubbles, but are very rarely observed with gas released from microbubbles. The simultaneous occurrence of gas release and expansion indicates that phase differences of the primary sound field were negligible in the field of view. This is the first study showing gas release from crushed bioactive glass and subsequent bubble dynamics. It should be noted that thermal pretreatment of the glass might alter the results. In previous studies, jetting was observed near free or solid interfaces and between bubble pairs.[20,21] The kind of jetting observed in Fig. 3 is bubble-pair jetting.

In conclusion, we observed the chipping-off of solid bioactive glass and a needle jet within released gas. This study provides experimental evidence that the glass observed to sink is associated to gas release. Gas release happens only during high-amplitude ultrasound pulses.

Acknowledgments This work was supported by JSPS KAKENHI, Grant No. JP17H00864 and JP20H04542, by the National Research Foundation of South Africa, Grant No. 127102, and by the Academy of Finland, Grant No. 340026.

ORCID iDs Michiel Postema https://orcid.org/0000-0001-5887-1739 Craig S. Carlson https://orcid.org/0000-0003-1059-1601 Nicole Anderton https://orcid.org/0000-0001-7114-2231 Laeticia Petit https://orcid.org/0000-0002-1673-8996 Jonathan Massera https://orcid.org/0000-0002-1099-8420 Nobuki Kudo https://orcid.org/0000-0003-3463-3714

1) L. L. Hench, J. Mater. Sci. Mater. Med. **17**, 967 (2006).
2) M. Ojansivu et al., PLoS One **13**, e0202740 (2018).
3) A. Houaoui et al., Biomolecules **11**, 444 (2021).
4) M. Postema et al., Proc. 44th UltraSonic Electronics Symp., 2023, 3P5, https://www.use-dl.org/2023/proceedings/pdf/3P5-9.pdf.
5) I. C. Macedo and W.-J. Yang, Jpn. J. Appl. Phys. **11**, 1124 (1972).
6) W. Soliman, T. Nakano, N. Takada, and K. Sasaki, Jpn. J. Appl. Phys. **49**, 116202 (2010).
7) N. Anderton et al., Jpn. J. Appl. Phys. **61**, SG8001 (2022).
8) E. Stride and N. Saffari, IEEE Trans. Ultrason. Ferroelectr. Freq. Control **52**, 2332 (2005).
9) T. Kanagawa, M. Honda, and Y. Kikuchi, Phys. Fluids **35**, 023303 (2023).
10) Y. Kikuchi, T. Kanagawa, and T. Ayukai, Chem. Eng. Sci. **269**, 117541 (2023).
11) C. S. Carlson, R. Matsumoto, K. Fushino, M. Shinzato, N. Kudo, and M. Postema, Jpn. J. Appl. Phys. **60**, SDDA06 (2021).
12) N. Anderton, C. S. Carlson, V. Aharonson, and M. Postema, Curr. Dir. Biomed. Eng. **8**, 781 (2022).
13) A. A. Doinikov and P. A. Dayton, J. Acoust. Soc. Am. **120**, 661 (2006).
14) C. E. Brennen, J. Fluid Mech. **472**, 153 (2002).
15) M. Postema, P. Marmottant, C. T. Lancée, M. Versluis, S. Hilgenfeldt, and N. de Jong, Proc. IEEE Ultrason. Symp., 2004, p. 1.
16) Y. Tomita and A. Shima, J. Fluid Mech. **169**, 535 (1986).
17) T. Kodama and K. Takayama, Ultrasound Med. Biol. **24**, 723 (1998).
18) C.-D. Ohl and R. Ikink, Phys. Rev. Lett. **90**, 214502 (2003).
19) X.-M. Liu, J. He, J. Lu, and X.-W. Ni, Jpn. J. Appl. Phys. **48**, 016504 (2009).
20) B. Biller, N. Hoppe, S. Adami, and N. A. Adams, Phys. Fluids **34**, 076111 (2022).
21) F. Reuter and C.-D. Ohl, Appl. Phys. Lett. **118**, 134103 (2021).
22) T. Moriyama, S. Yoshizawa, and S.-I. Umemura, Jpn. J. Appl. Phys. **51**, 07GF27 (2012).
23) T. Aikawa and N. Kudo, Jpn. J. Appl. Phys. **60**, SDDD3 (2021).
24) N. Obara, S.-I. Umemura, and S. Yoshizawa, Jpn. J. Appl. Phys. **60**, SDDE04 (2021).
25) N. Kudo et al., Jpn. J. Appl. Phys. **59**, SKKE02 (2020).
26) N. Kudo, IEEE Trans. Ultrason. Ferroelectr. Freq. Control **64**, 273 (2017).